

**TECHNICAL NOTE****CRIMINALISTICS***John W. Bond,<sup>1,2</sup> D.Phil*

## Optical Enhancement of Fingerprint Deposits on Brass Using Digital Color Mapping

**ABSTRACT:** The reflection of visible light from  $\alpha$ -phase brass subject to surface oxidation in air at elevated temperatures is investigated. X-ray photoelectron and auger electron spectroscopy confirm that covered areas of brass (not exposed to air) display dezincification but an absence of significant surface oxidation, confirming a differential oxidation mechanism. Visualization of differential oxidation is shown to be enhanced by selective digital mapping of colors reflected from the surface of the brass using Adobe® Photoshop®. Enhancement is optimal when the brass is heated to  $\sim 250^\circ\text{C}$  with areas of oxidation having a mirror-like appearance. The use of this enhancement method to produce a faithful image of fingerprint ridge characteristics is demonstrated on brass shell casings where fingerprints were deposited prefiring.

**KEYWORDS:** forensic science, latent fingerprint, print visualization, metal corrosion, electrochemical mechanism, optical enhancement

Recent research has shown how fingerprint patterns deposited as sweat on brass shell casings can be visualized as a result of an electrochemical reaction between the sweat deposit and brass (1–5). This reaction can lead to the formation of a rectifying Schottky barrier contact between p-type copper (I) oxide or n-type zinc oxide corrosion formed on the surface of the brass and the brass substrate (6,7). When this occurs, a potential ( $V$ ) applied to the brass has been shown to vary exponentially with that measured on an area of fingerprint sweat corrosion, with a potential difference ( $\Delta V$ ) of up to  $\sim 10$  V for  $V = 1400$  V (6). With  $\Delta V$  of this magnitude, a fine carbon powder (particle size  $\sim 10$   $\mu\text{m}$ ) introduced to the brass has been found to adhere preferentially to areas of corrosion, thus enabling the fingerprint to be visualized (4,5). Such visualization has been achieved even after the sweat deposit has been removed from the brass (8).

Lately, Wightman, and O'Connor (9) have investigated the visualization of fingerprints deposited on planar brass, aluminum, and stainless steel disks that were heated subsequently to temperatures between 200 and 900°C. They confirmed results from earlier work related to fingerprint visualization on heated metals (4) with, frequently, no additional enhancement (such as that described above) being necessary to visualize the fingerprint ridge characteristics. They postulated that visualization occurred owing to differential oxidation; that is, the fingerprint sweat acted as a barrier to oxidation on those parts of the metal surface covered by the sweat. Wightman and O'Connor (9) believed that visualization was enhanced by interference colors resulting from a thin oxide film on the metal surface not covered by the sweat. Enhancement through optical interference has been observed previously for fingerprints deposited on brass disks in Iraq (10), where the increased air

temperature (relative to the U.K.) resulted in a zinc oxide layer that produced optical interference as the viewing angle of the disk was adjusted in natural daylight. The thickness ( $t$ ) of this zinc oxide film was found to be  $70\text{ nm} \leq t \leq 80\text{ nm}$ , which is consistent with values reported for zinc oxide formed during the electrochemical corrosion of  $\alpha$ -phase brass in an aqueous saline solution (11).

Optical interference and differential oxidation present noninvasive methods of visualizing fingerprint deposits and fingerprint corrosion on metal, which can have benefits over techniques that require physical or chemical interaction with the fingerprint or substrate (12–15).

In this technical note, we examine how the visualization of differential oxidation on heated  $\alpha$ -phase brass can be enhanced by digital mapping of colors reflected from the surface of the brass. We identify the temperature to which the brass needs to be heated to achieve an optimum enhancement in visualization by this method and examine the surface composition of areas subject to differential oxidation using X-ray photoelectron (XPS) and auger electron spectroscopy (AES). Digital mapping of colors is then applied to brass disks subject to fingerprint deposition and subsequent heating and finally to brass shell casings where fingerprints were deposited prefiring. Digital color mapping is shown to produce a faithful image of the fingerprint ridge characteristics on brass shell casings.

### Experimental Details

#### *Materials and Method*

Initially, differential oxidation was explored by heating 1-mm-thick, 25-mm-diameter  $\alpha$ -phase brass disks (68Cu–32Zn by percentage weight) onto which another brass disk had been partially overlaid. The additional (overlying) brass disk provided an area that prevented oxygen from the air reaching the disk surface but which would reach the same temperature as the disk during heating. Disks were heated to a temperature ( $T$ ) of between 50 and 600°C in 50°C intervals. Each disk was held over a Bunsen flame until the required temperature had been reached (typically a few

<sup>1</sup>Northamptonshire Police, Force HQ, Wootton Hall, Northampton, NN4 0JQ, U.K.

<sup>2</sup>Forensic Research Centre, University of Leicester, Leicester, LE1 7EA, U.K.

Received 21 July 2010; and in revised form 20 Sept. 2010; accepted 3 Oct. 2010.

minutes). Each disk was then allowed to cool in air. The temperature was measured by means of a K-type thermocouple placed in contact with the disk (Hanna Instruments, Leighton Buzzard, U.K.). The experiments were then repeated with a fingerprint deposit replacing the overlaying disk, five donors each providing a fingerprint for each temperature which gave 60 samples in total (12 temperatures  $\times$  five donors). Fingerprints were deposited by pressing a finger onto the brass surface for 1–2 sec with a light pressure sufficient to ensure contact between the finger and brass. While no attempt was made to regulate the amount of pressure applied by individuals, this procedure was intended to produce reasonably uniform deposition. All fingerprint donors washed their hands with soap and water 20 min prior to depositing fingerprints, and no artificial stimulation of sweat was employed such as placing the hand in a plastic bag (16) or wearing a latex glove prior to deposition (14).

Finally, 40 brass 9-mm pistol cartridges were washed in distilled water followed by a wash in acetone and finally another wash in distilled water prior to drying with a paper towel. Each cartridge was handled by one of the 40 donors to leave one or more fingerprints on the cartridges. The cartridges were then loaded into magazines, which were inserted into a pistol and discharged. When fired, each cartridge was automatically ejected from the magazine. Digital color mapping was performed using Adobe® Photoshop® CS4, version 11.0 (17).

XPS/AES was performed using a VG ESCALab 200d spectrometer (VG Scienta, Hastings, U.K.), Al K  $\alpha$  radiation (1486.6 eV), and a hemispherical analyzer. Individual high-resolution spectra were taken at a pass energy of 50 eV and an energy step of 0.05 eV.

## Results and Discussion

Overlaid disks showed varying visibility of the area beneath the overlay, which depended on the temperature reached by the disk. For disks, where  $T > 300^\circ\text{C}$ , the area of overlay was clearly visible. For  $T < 300^\circ\text{C}$ , disks were photographed in natural daylight and the resulting image analyzed with the Hue/Saturation dialog box in Adobe® Photoshop®. Specifically, the overlaid and nonoverlaid areas on each disk were color deconvoluted using the red, green, and blue (R/G/B) color model (17). With 32-bit mapping, the R/G/B contributions to the reflected light showed little variation between the two areas for  $50^\circ\text{C} \leq T \leq 200^\circ\text{C}$ . The largest variation occurred for  $T = 250^\circ\text{C}$ , where (on a scale of 0–1) R/G/B was 0.83:0.86:0.83 and 0.82:0.8:0.34 for the nonoverlaid and overlaid areas, respectively. Thus (with  $T = 250^\circ\text{C}$ ), the blue contribution was less for the overlaid area. This is what might be expected as the overlaid area would (through differential oxidation) exhibit less oxidation and therefore retain more of the natural yellow appearance of metallic brass with red and green giving the reflected yellow color (9,17). The nonoverlaid area appeared to have a mirror-like finish with a white appearance when viewed obliquely. Again, this white appearance would be expected as the R/G/B values were similar. Oxidized brass with this appearance was also observed by Wightman and O'Connor (9), which they referred to as the brass "turning silver." Wightman and O'Connor also found a decline in fingerprint visualization between 200 and  $280^\circ\text{C}$  (9).

XPS/AES analyses of both overlaid and nonoverlaid areas of each disk are shown in Table 1. It can be seen that the Zn/Cu ratio is similar for both areas demonstrating that heating the brass causes a movement of zinc toward the surface of the metal irrespective of whether it is able to be oxidized at the surface. This migration has been observed previously for heated  $\alpha$ -phase brass (18), and it is

TABLE 1—X-ray photoelectron/ Auger electron spectroscopy analysis of nonoverlaid and overlaid areas of heated  $\alpha$ -phase brass disks.

Disk Temperature (°C)	Nonoverlaid Area			Overlaid Area		
	Zn/Cu	Zn Present as	Cu Present as	Zn/Cu	Zn Present as	Cu Present as
50	1:3.12	Zn and ZnO	Cu and Cu <sub>2</sub> O	1:2.2	Zn	Cu
100	1:2.1	Zn and ZnO	Cu and Cu <sub>2</sub> O	1:2.2	Zn	Cu
150	1:2.1	ZnO	Cu and Cu <sub>2</sub> O	1:2.1	Zn	Cu
200	1:1.7	ZnO	Cu <sub>2</sub> O	1:1.8	Zn and ZnO	Cu
250	1:1.6	ZnO	Cu <sub>2</sub> O	1:1.6	Zn and ZnO	Cu and Cu <sub>2</sub> O
300	1:1.2	ZnO	Cu <sub>2</sub> O and CuO	1:1.3	Zn and ZnO	Cu and Cu <sub>2</sub> O
350	1:1.1	ZnO	Cu <sub>2</sub> O and CuO	1:1.1	Zn and ZnO	Cu and Cu <sub>2</sub> O
400	1:1.2	ZnO	Cu <sub>2</sub> O and CuO	1:1.1	Zn and ZnO	Cu and Cu <sub>2</sub> O
450	1:0.9	ZnO	CuO	1:0.9	Zn and ZnO	Cu and Cu <sub>2</sub> O
500	1:0.9	ZnO	CuO	1:0.8	Zn and ZnO	Cu and Cu <sub>2</sub> O
550	1:0.8	ZnO	CuO	1:0.8	Zn and ZnO	Cu and Cu <sub>2</sub> O
600	1:0.8	ZnO	CuO	1:0.8	Zn and ZnO	Cu and Cu <sub>2</sub> O

well known that dezincification (the loss of zinc) is accelerated as temperature increases (19). Metallic zinc and copper were present on the surface of the overlaid area at higher temperatures than on the nonoverlaid area and, while oxides of both elements were present in both areas, AES showed the concentration of zinc and copper atoms to be much greater than the concentration of ions in the overlaid area. This, therefore, confirms the differential oxidation mechanism proposed by Wightman and O'Connor (9).

To seek to improve the visualization of the overlaid area, the yellow part of the spectrum was color mapped on the  $T = 250^\circ\text{C}$  disk. As the Hue values in Adobe® Photoshop® are based on a  $360^\circ$  color spectrum or "wheel" (Fig. 1), mapping was undertaken for  $45^\circ \leq \theta \leq 75^\circ$  where  $\theta$  is the color wheel angle (Fig. 1). It was found that optimum enhancement in visualization of the overlaid area occurred for a change of  $\theta$  of  $-60^\circ$ , that is, mapping to the red part of the spectrum. Figure 2 shows the overlaid disk heated to  $250^\circ\text{C}$ , before and after mapping, the dashed line showing the location of the overlaying disk, which has been removed. It can be seen that there has been some creeping of oxidation under the overlaying disk, which, clearly, would be a problem if this were to occur when seeking to enhance and identify fingerprint ridge characteristics by mapping. This is considered later.

Experiments with a fingerprint deposit replacing the overlaying disk gave similar results with all five disks heated to  $T = 250^\circ\text{C}$  producing the most improved visualization; Fig. 3 showing a typical disk for  $T = 250^\circ\text{C}$  before and after color mapping of  $45^\circ \leq \theta \leq 75^\circ$  by a change of  $\theta$  of  $-60^\circ$ . Here, there is no obvious creep of oxidation into areas of disk covered by the fingerprint sweat deposit (as was observed in Fig. 2), and it is likely that the fingerprint sweat provides a better seal to the surface of the brass than an overlaying disk. It is known that sebum-rich fingerprints, containing fatty acids and sterols, are adsorbed from solution onto metals to form closely packed monolayers (20).

Of the 40 discharged shell casings, six showed signs of fingerprint ridges and, for four of these, the ridge detail appeared in an

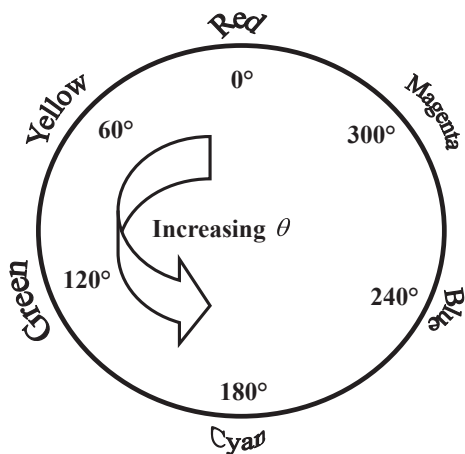


FIG. 1—360° color spectrum or wheel.

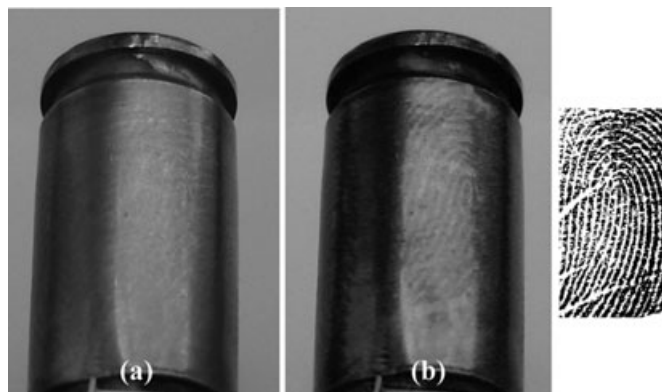


FIG. 4—Fingerprint deposited on a brass shell casing prefiring shown postfiring. (a) Shows the casing before and (b) after digital color mapping. Inset: an inked impression of the fingerprint.

generally toward the flat base of the casing where mechanical friction by the pistol ejection mechanism is less (3). However, this is not so here. Consistent with the fingerprints deposited on planar disks, there is no evidence of oxidation creeping into areas of disk covered by the fingerprint sweat deposit. The inset in Fig. 4 is of an inked impression of the fingerprint which a registered expert confirmed the commonality of ridge characteristics between the color-mapped image and inked impression.

**Conclusion**

Through XPS/AES surface analyses of areas of  $\alpha$ -phase brass subject to elevated temperatures, it is confirmed the differential oxidation mechanism proposed by Wightman and O'Connor (9). Further, it is shown how the visibility of this differential oxidation can be enhanced by selective digital color mapping of the yellow part of the visible spectrum. The enhancement obtained is optimal when the brass is heated to  $\sim 250^{\circ}\text{C}$  with areas of oxidation having a mirror-like appearance. The use of this enhancement method to produce a faithful image of fingerprint ridge characteristics has been demonstrated on brass shell casings. The success of this technique would seem to depend critically on the degree of oxidation of areas not covered by the fingerprint sweat deposit and the thickness of the resulting zinc oxide thin film.

*Acknowledgments*

The author is indebted to the many members of Northamptonshire Police who donated willingly their latent fingerprints for this research. The assistance of Mrs. Trudy Loe (Research Officer Northamptonshire Police) with the preparation of the manuscript is acknowledged with thanks. The support of the Chief Officers of Northamptonshire Police in enabling this research to have been conducted is gratefully acknowledged.

**References**

1. Williams G, McMurray HN, Worsley DA. Latent fingerprint detection using a scanning Kelvin microprobe. *J Forensic Sci* 2001;46:1085–92.
2. Williams G, McMurray N. Latent fingerprint visualization using a scanning Kelvin probe. *Forensic Sci Int* 2007;167:102–9.
3. Williams G. Visualization of fingerprints on metal surfaces using a scanning kelvin probe. *Fingerprint World* 2010;36:51–60.
4. Bond JW. Visualization of latent fingerprint corrosion of metallic surfaces. *J Forensic Sci* 2008;53:812–22.

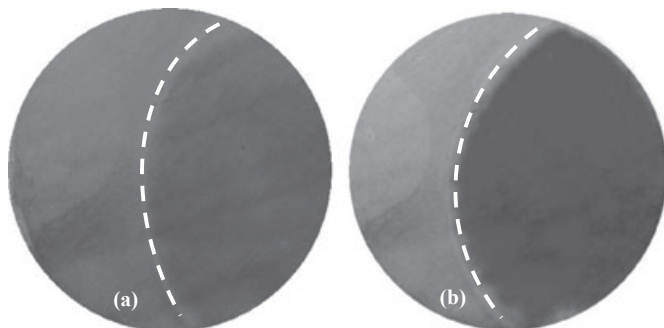


FIG. 2—Brass disk heated to  $T = 250^{\circ}\text{C}$ . The overlaying disk (removed) lay to the right of the dashed line. (a) Shows the disk before and (b) after digital color mapping.

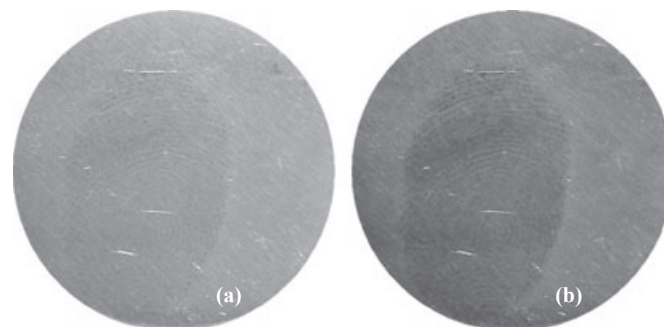


FIG. 3—Fingerprint deposited on a brass disk heated subsequently to  $T = 250^{\circ}\text{C}$ . (a) Shows the disk before and (b) after digital color mapping.

area that manifested the mirror-like appearance described earlier. Observing fingerprints for this number of discharged shell casings are consistent with previous work (3,4), and the relatively low success rate is thought to be associated with heat and friction damage (3,4). All six casings were photographed in natural daylight and the color mapping referred to previously applied. The four casings displaying the mirror-like appearance all showed an improvement in fingerprint ridge visibility; Fig. 4 showing a typical example. It can be seen from Fig. 4 that the fingerprint covers an area that runs along the length of the casing. It has been proposed previously that recovered fingerprints on discharged shell casings are located

5. Bond JW, Heidel C. Visualization of latent fingerprint corrosion on a discharged brass shell casing. *J Forensic Sci* 2009;54:892–4.
6. Bond JW. On the electrical characteristics of latent finger mark corrosion of brass. *J Phys D Appl Phys* 2008;41:125502.
7. Bond JW. Determination of the characteristics of a Schottky barrier formed by latent finger mark corrosion of brass. *J Phys D Appl Phys* 2009;42:235301.
8. Bond JW. Imaging fingerprint corrosion on fired brass shell casings. *Rev Sci Instrum* 2009;80:075108.
9. Wightman G, O'Connor D. The thermal visualization of latent fingerprints on metallic surfaces. *Forensic Sci Int* 2011;204:88–96.
10. Bond JW, Eliopoulos LN, Brady TF. Visualization of latent fingerprint corrosion of brass, climatic influence in a comparison between the UK and Iraq. *J Forensic Sci* 2011;56(2):506–9.
11. Kosec T, Merl DK, Milosev I. Impedance and XPS study of benzotriazole films formed on copper, copper-zinc alloys and zinc in chloride solution. *Corros Sci* 2008;50:1987–97.
12. Crane NJ, Bartick EG, Perlman RS, Huffman S. Infrared spectroscopic imaging for non-invasive detection of latent fingerprints. *J Forensic Sci* 2007;52:48–53.
13. Tahtouh M, Despland P, Simmon R, Kalman JR, Reedy BJ. The application of infrared chemical imaging to the detection and enhancement of latent fingerprints: method optimization and further findings. *J Forensic Sci* 2007;52:1089–96.
14. Worley CG, Wiltshire SS, Miller TC, Havrilla GJ, Majidi V. Detection of visible and latent fingerprints using micro-x-ray fluorescence elemental imaging. *J Forensic Sci* 2006;51:57–63.
15. Dubey SK, Anna T, Shakher C, Mehta DS. Fingerprint detection using full-field swept-source optical coherence tomography. *Appl Phys Lett* 2007;91:181106.
16. Migron Y, Hocheerman G, Springer E, Almog J, Mandler D. Visualization of sebaceous fingerprints on fired cartridge cases: a laboratory study. *J Forensic Sci* 1998;43:543–8.
17. Evening M. Adobe® Photoshop® CS3 for photographers. Oxford, UK: Elsevier, 2007.
18. Beucher E, Lefez B, Lenglet M. Optical determination of cuprous oxide at zinc oxide-metal interface of an oxidized  $\alpha$  brass. *Phys Status Solidi (A)* 1993;136:139–44.
19. Trethewey K, Chamberlain J. Corrosion for science and engineering. Harlow, UK: Addison Wesley Longman, 1998.
20. Scruton B, Robins BW, Blott BH. The deposition of fingerprint films. *J Phys D Appl Phys* 1975;8:714–23.

## Additional information and reprint requests:

John W. Bond, D.Phil.  
Scientific Support Department  
Northamptonshire Police  
Wootton Hall  
Northampton NN4 OJQ  
U.K.  
E-mail: john.bond@northants.police.uk